

Electronic Supplementary Information (ESI[†])

Nb/Se Co-doped BiOI Nanomaterials with Exposed (110) Facets for Enhanced Visible-Light-Driven Photocatalytic Activity

Yifeng Xu^{1,2}, Aihua Yan^{1,2,*}, Xiaohui Zhang², Fei Huang^{1,3*}, Dengke Li², Xianhui Zhao², Haifeng Weng², Zhuoyu Zhang²

¹Low Carbon Energy Institute, China University of Mining and Technology, Xuzhou 221008, China

²School of Materials and Physics, China University of Mining and Technology, Xuzhou 221116, China

³Jiangsu Key Laboratory of Coal-based Greenhouse Gas Control and Utilization, China University of Mining and Technology, Xuzhou 221008, China

* **Corresponding authors.** Tel: +86-516-83883501

Email: yanaihua111@163.com (Aihua Yan) and huangfei7804@163.com (Fei Huang)

1. Experimental Section

1.1 Raw Materials and Chemicals

Potassium Iodide (KI, ≥ 99%, AR) was purchased from Aladdin. Bismuth nitrate pentahydrate ($\text{Bi}(\text{NO}_3)_3 \cdot 5\text{H}_2\text{O}$, 99.999%, GR), and Niobium diselenide (NbSe_2 , 99.8%) were obtained from Alfa Aesar. Ethylene glycol ($\text{C}_2\text{H}_6\text{O}_2$, AR) was supplied by Sinopharm Chemical Reagent Co., Ltd. All chemicals were used without further purification.

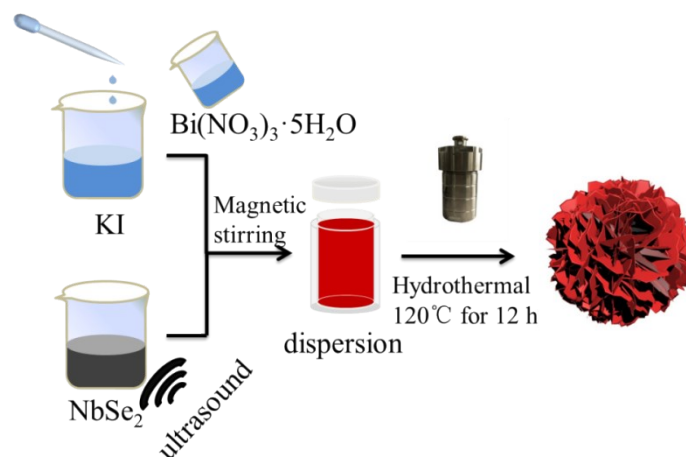


Fig. S1 Schematic preparation process of NSC-BOI-x hybrids

1.2 Preparation of NSC-BOI

The preparation procedure of NSC-BOI-x samples was shown in **Fig. S1**. Typically, 3 mmol $\text{Bi}(\text{NO}_3)_3 \cdot 5\text{H}_2\text{O}$ and 3 mmol KI were added into 20 mL ethylene glycol, respectively. Then, above solutions were magnetically stirred to form transparent and homogeneous solutions. The $\text{Bi}(\text{NO}_3)_3 \cdot 5\text{H}_2\text{O}$ solution was dropwise added into KI solution. Afterwards, a certain amount of NbSe_2 was dispersed into 40 mL ethylene glycol, ultrasonically treated and transferred into above mixed solution. Subsequently, the suspension continued to magnetically stir at room temperature for an hour, then transferred to a 100 mL teflon-lined autoclave, sealed, maintained at 120 °C for 12 h, naturally cooled to room temperature. The final products were collected by centrifugation, washed with deionized water and absolute ethanol for several times, and dried at 60 °C for 12 h. For convenience, final samples with different mole ratio were labeled as NSC-BOI-x (x=0.2, 1.0, 1.5, 2.0, 2.5, 3.0).

1.3 Characterization of Materials

The crystal phase of the samples was identified by X-ray diffractometer (XRD, D8 advanced, Bruker) with Cu $K\alpha$ radiation. The scan rate was 5 °/min range in the range of 10°-90°. The molecular structure was analyzed by a Raman spectrometer (Senterra, Bruker) with 532 nm wavelength excitation at room temperature. Morphological changes and surface microstructure were observed through field emission scanning electron microscopy (FESEM, MAIA3 LMH, Tescan), equipped with an energy-dispersive spectrometer accessory. The microstructure construction was recorded by transmission electron microscopy (TEM, Tecnai G2 F20, FEI) with 200 kV accelerating voltage. Electron spin-resonance (ESR) test was carried out in the X-band (9 GHz) with 0.4 mT modulation width and a magnetic field modulation of 100 kHz using a Japan, JES-FA200 EPR spectrometer at room temperature. Chemical states and surface elements were characterized by X-ray photoelectron spectrometer (XPS, ESCALAB 250Xi, Thermo Fisher) with an Al $K\alpha$ source. The UV-vis spectrophotometer (Lambda 950, PerkinElmer) with the spectral range of 190~1100 nm and 150 mm integrating ball was used to record absorption spectra. Photoluminescence (PL) spectra were characterized by a fluorescence spectrometer (F-7000, Hitachi) under 385 nm wavelength excitation. Electrochemical impedance spectroscopy (EIS) and transient photocurrent spectra were performed on an electrochemical work station (CHI660E, Shanghai CH Instruments) equipped with a Xenon lamp (CHF-XM-500W), using the samples as the working electrode, Pt sheet as the counter electrode and calomel electrode as the reference electrode.

1.4 Photocatalytic Measurements

The photocatalytic activity of as-synthesized BOI and NSC-BOI photocatalysts was evaluated by degrading RhB aqueous solution under visible-light irradiation ($380 \text{ nm} \leq \lambda \leq 780 \text{ nm}$). The light source came from a xenon lamp with two cutoff filters (JB380 and VISREF 350-780). In detail, 30 mg as-prepared samples were added into 200 mL RhB aqueous solution ($15 \text{ mg}\cdot\text{L}^{-1}$). The mixture kept stirring for 1 h in dark to achieve adsorption-desorption equilibrium. During the irradiation, 5 mL solution was taken out at an interval of 10 min and centrifuged for 3 min at 9000 rpm to remove the photocatalyst. The concentration of the supernatant was monitored according to the changes of absorbance at the wavelength of 555 nm. The degradation efficiency (η , %) was calculated as follows:

$$\eta (\%) = (C_0 - C_t) / C_0 \times 100\% \quad (1)$$

where C_0 represents initial adsorption-desorption concentration and C_t represents the concentration of RhB solution after irradiation.

2. SEM Image

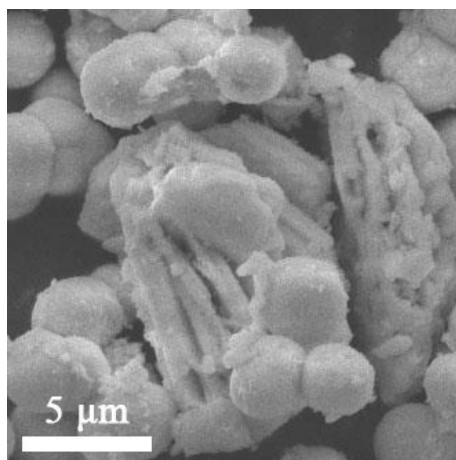


Fig. S2 SEM image of NSC-BOI-5.0 samples

3. ESR spectrum

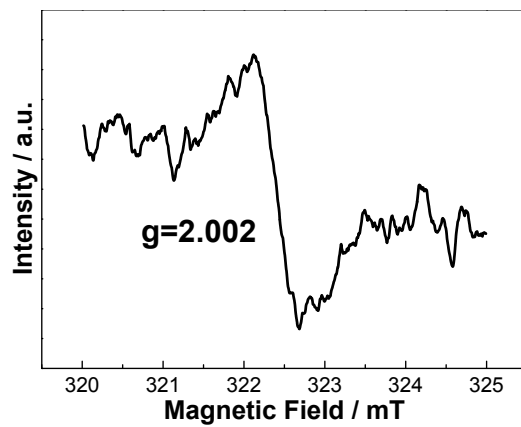


Fig. S3 ESR spectrum of NSC-BOI-2.0 samples

4. Peak Intensity Ratio

Table S1 Peak intensity ratio between (110) crystal plane and (120) crystal plane

X values in NSC-BOI-x samples	Peak intensity ratio
0	1.00
1.0	1.21
2.0	1.32
3.0	1.05

5. XPS Analysis

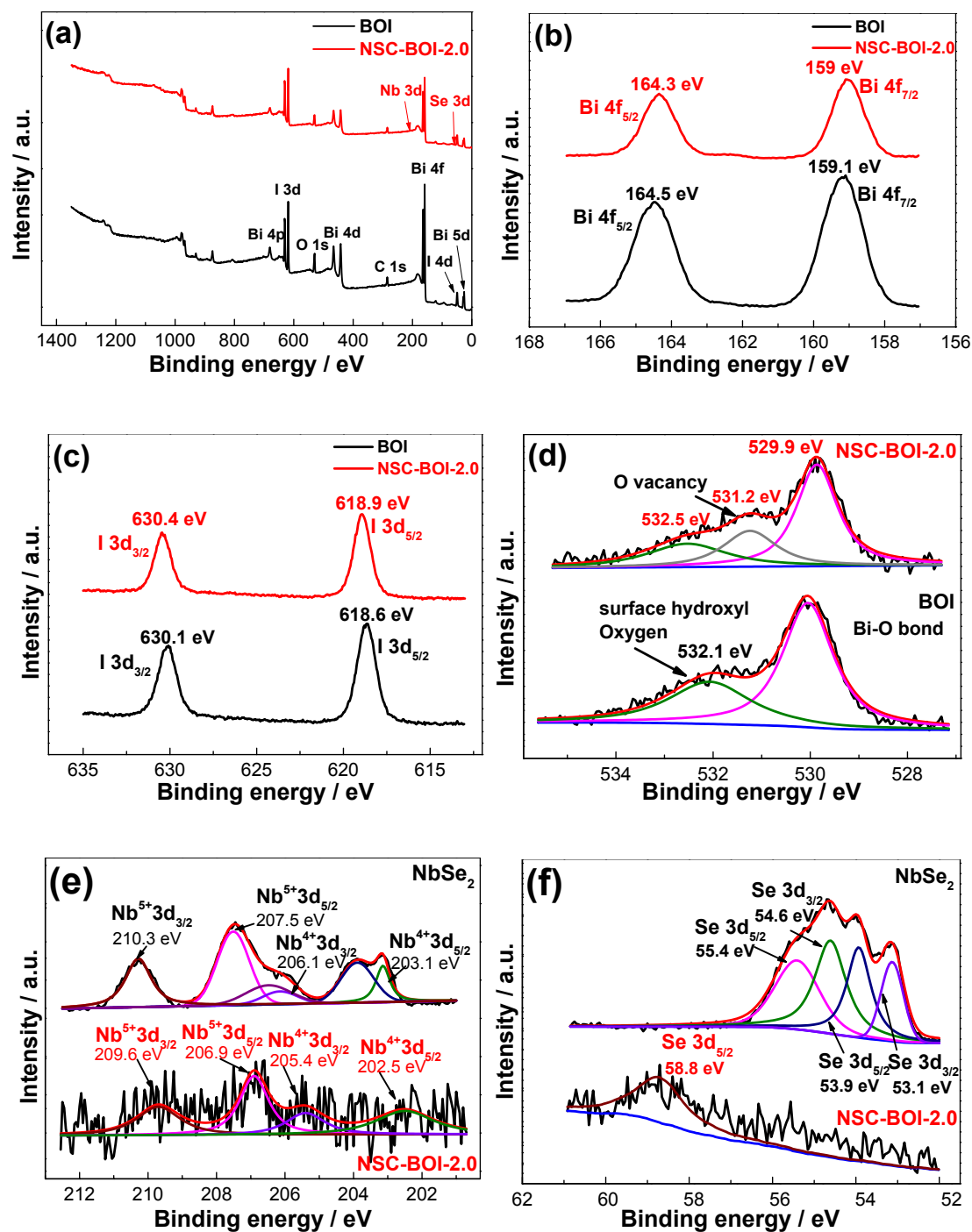


Fig. S4 XPS spectra of pure BOI and NSC-BOI-2.0 samples. (a) Wide scan; narrow scan of (b) Bi 4f, (c) I 3d, (d) O 1s, (e) Nb 3d and (f) Se 3d.

6. Calculated Absorption Edges and Band Gaps

Table S2 Summary of absorption edges and band gaps of NSC-BOI-x samples

X values in NSC-BOI-x samples	Absorption edges / nm	Band gaps / eV
0	655	1.89
0.2	645	1.92
1.0	631	1.96
1.5	628	1.97
2.0	621	1.99
2.5	618	2.0
3.0	604	2.05

7. Equilibrium Concentration and Specific Surface Area

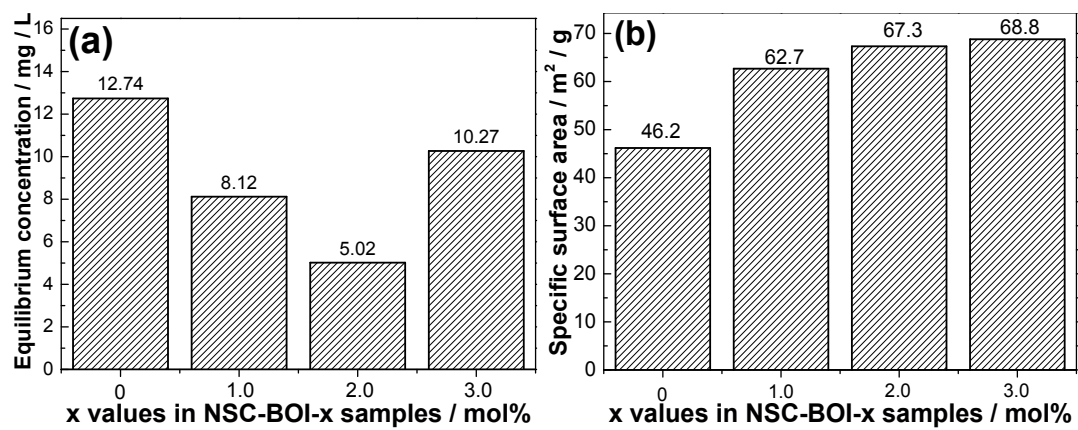


Fig. S5 (a) Equilibrium concentration of different samples in dark for a hour; (b) specific surface area of different samples.

8. ESR Spectra

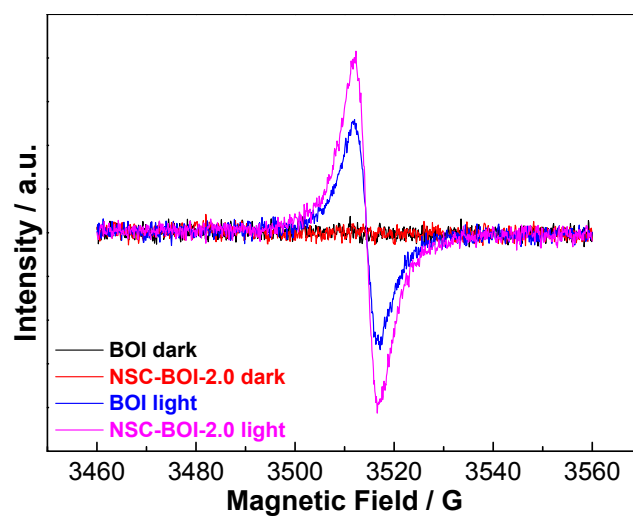


Fig. S6 ESR spectra of DMPO-h⁺ with NSC-BOI-2.0 samples under visible light irradiation.

9. Calculated Flat Band Potential and Band gap

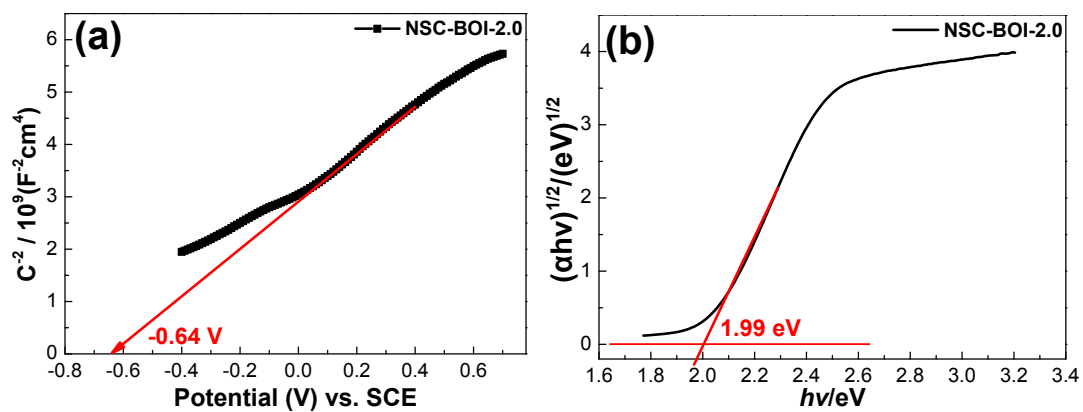


Fig. S7 (a) Mott-Schottky plots of NSC-BOI-2.0 samples obtained in dark and 0.1 M Na_2SO_4 electrolytes; (b) $(\alpha h\nu)^{1/2}$ vs. $h\nu$ curve of NSC-BOI-2.0 samples